ResearchGate

See discussions, stats, and author profiles for this publication at: https://www.researchgate.net/publication/231526024

Molecular Recognition of Aqueous Dipeptides at Multiple Hydrogen-Bonding Sites of Mixed Peptide Monolayers

ARTICLE *in* JOURNAL OF THE AMERICAN CHEMICAL SOCIETY · OCTOBER 1996

Impact Factor: 12.11 · DOI: 10.1021/ja961526f

CITATIONS
90

READS
8

3 AUTHORS:

Xiao Zha
Sichuan Tumor Hospital and Institute
41 PUBLICATIONS **667** CITATIONS
SEE PROFILE

Katsuhiko Ariga
National Institute for Materials Science
623 PUBLICATIONS **21,476** CITATIONS
SEE PROFILE

Toyoki Kunitake
FAIS
672 PUBLICATIONS **20,611** CITATIONS
SEE PROFILE

Available from: Xiao Zha
Retrieved on: 24 January 2016

Molecular Recognition of Aqueous Dipeptides at Multiple Hydrogen-Bonding Sites of Mixed Peptide Monolayers

Xiao Cha,[†] Katsuhiko Ariga, and Toyoki Kunitake*[,‡]

Contribution from the Supermolecules Project, JRDC, 2432 Aikawa, Kurume Research Park, Kurume, 839 Japan

Received May 7, 1996[⊗]

Abstract: Oligopeptide amphiphiles with different dipeptide moieties of $-XYNH_2$ (X = Gly and Ala, Y = Gly, Ala, Val, Leu, and Phe) were synthesized. Binding of aqueous dipeptides onto monolayers of equimolar mixtures of these amphiphiles with a benzoic acid amphiphile ($2C_{18}BCOOH$) was investigated by $\pi-A$ isotherm measurement, FT-IR spectroscopy, and XPS elemental analysis. For given GlyX dipeptides (X = neutral and hydrophobic residues), the binding ratio was lessened with increasing sizes of the side chain of the Y residue in the GlyY dipeptide moiety of the host amphiphiles. The Langmuir-type saturation behavior was observed for binding of GlyLeu to an equimolar monolayer of $2C_{18}BGly_2NH_2$ and $2C_{18}BCOOH$. Its binding constant of 475 M^{-1} was 10 times larger than that observed for a single-component monolayer of $2C_{18}BGly_2NH_2$ ($K = 35$ M^{-1}). The saturation guest/host ratio was 0.47. The mode of substrate insertion into the binding site was examined by FT-IR spectroscopy. When the hydrophobic residue was on the C-terminal of a guest dipeptide (GlyX), the C-terminal insertion was selected with accompanying formation of cyclic carboxylic acid dimers at the interface. In the case of XGly guests, the N-terminal insertion with salt bridge formation with the host was observed. When the two residues of a dipeptide had close hydrophobicities, both C- and N-terminal insertions were observed. Formation of these binding sites is apparently induced by dipeptide binding.

Introduction

Molecular recognition between signal peptides and receptor proteins is a basic feature of many biological processes.[1−3] These receptors are usually located on the biomembrane surface. How to mimic these processes and design artificial peptide receptors has intrigued many chemists,[4−6] because of their practical applications in addition to their use as a tool to study natural receptor processes.

It has been reported that an ordered array of functional groups formed at the interface controls binding of amino acids and subsequent crystal growth.[7] More recently, Higashi *et al.* reported enantioselective binding of α-amino acids by a poly-(L-glutamic acid)-functionalized monolayer.[8] These examples suggest that functional arrays formed at the air−water interface are useful for selective peptide binding. In order to develop peptide receptors at the artificial interface, we have been investigating specific binding of aqueous dipeptides onto peptide-functionalized monolayers. Peptide binding was not detectable in the case of monolayers of single-chain derivatives of oligoglycines.[9] In this case, strong inter-peptide hydrogen bonding prevented binding of guest peptides. Very recently, we have shown that aqueous dipeptides such as GlyX can be selectively bound to the monolayer of an amphiphile in which the dioctadecylamine moiety was connected with the glycylglycinamide head group via the terephthaloyl unit ($2C_{18}BGly_2NH_2$; see Scheme 1).[10] In this system, selective binding of dipeptides was promoted by antiparallel hydrogen bonding and

Scheme 1

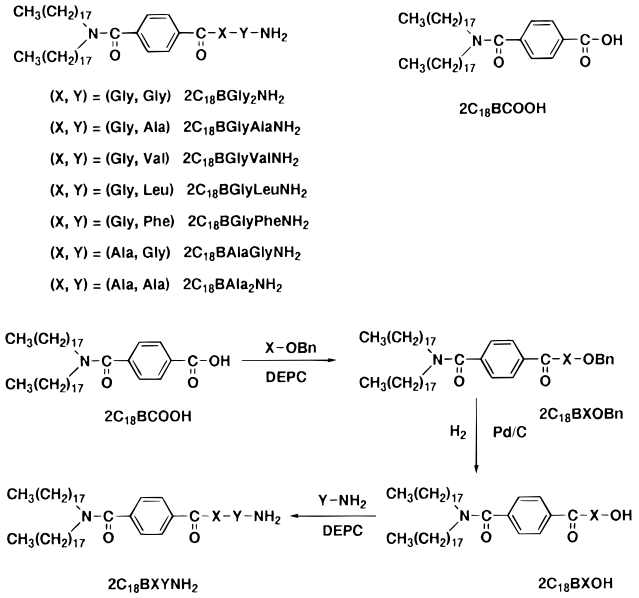

[†] Permanent address: Department of Biology, Sichuan Tumor Institute and Hospital Southern Train Station, Chengdu 610041, The People's Republic of China.

[‡] Permanent address: Faculty of Engineering, Kyushu University, Fukuoka 812, Japan.

[⊗] Abstract published in *Advance ACS Abstracts,* September 15, 1996.

(1) See, e.g.: Germain, R. N.; Margulies, D. H. *Annu. Rev. Immunol.* **1993**, *11*, 403.

(2) Stern, L. J.; Brown, J. H.; Jardetzky, T. S.; Gorga, J. C.; Urban, R. G.; Strominger, J. L.; Wiley, D. C. *Nature* **1994**, *368*, 215.

(3) Tame, J. R. H.; Murshudov, G. N.; Dodson, E. J.; Neil, T. K.; Dodson, G. G.; Higgins, C. F.; Wilkinson, A. J. *Science* **1994**, *264*, 1578.

(4) (a) Borchart, A.; Still, W. C. *J. Am. Chem. Soc.* **1994**, *116*, 373. (b) Torneiro, M.; Still, W. C. *J. Am. Chem. Soc.* **1995**, *117*, 5887.

(5) Albert, J. S.; Goodman, M. S.; Hamilton, A. D. *J. Am. Chem. Soc.* **1995**, *117*, 1143.

(6) Labrenz, S. R.; Kelly, J. W. *J. Am. Chem. Soc.* **1995**, *117*, 1655.

(7) (a) Gidalevitz, D.; Weissbuch, I.; Kjaer, K.; Als-Nielson, J.; Leiserowitz, *J. Am. Chem. Soc.* **1994**, *116*, 3271. (b) Landau, E. M.; Grayer Wolf, S.; Levanon, M.; Leiserowitz, L.; Lahav, M.; Sagiv, J. *J. Am. Chem. Soc.* **1989**, *111*, 1436.

(8) Higashi, N.; Saitou, M.; Mihara, T.; Niwa, M. *J. Chem. Soc., Chem. Commun.* **1995**, 2119.

(9) Cha, X.; Ariga, K.; Kunitake, T. *Bull. Chem. Soc. Jpn.* **1996**, *69*, 163.

(10) Cha, X.; Ariga, K.; Onda, M.; Kunitake, T. *J. Am. Chem. Soc.* **1995**, *117*, 11833.

S0002-7863(96)01526-0 CCC: $12.00 © 1996 American Chemical Society

hydrophobic interaction between host peptide units and guest dipeptides. However, the binding of XGly or XX′ dipeptides (X, X′ = neutral amino acid residues other than Gly) onto the $2C_{18}BGly_2NH_2$ monolayer is not detectable, probably because of steric crowding (for XX′ dipeptides) or weak parallel hydrogen bonding (for XGly dipeptides).[10] We need to develop new monolayer systems in order to prepare binding sites that are selective for these dipeptides. The nature of the binding cavity would be readily modified by using mixed monolayers. Short acidic or basic groups should be appropriate for forming new cavities upon mixing with oligopeptide polar groups, as we indicated in a preliminary publication.[11]

In this paper we present a full account of dipeptide recognition by mixed monolayers of oligopeptide amphiphiles ($2C_{18}$-$BXYNH_2$) and benzoic acid amphiphiles ($2C_{18}BCOOH$). The details of binding selectivity and the structure of the binding site are elucidated with the help of XPS analysis and FT-IR spectroscopy. The recognition site is self-assembled on the surface of the monolayer via the interaction with guest dipeptides. This is analogous to induced-fit phenomena at the active site of enzymes.

Experimental Section

Synthesis of Amphiphiles. Amphiphiles $2C_{18}BGlyAlaNH_2$, $2C_{18}$-$BGlyValNH_2$, $2C_{18}BGlyLeuNH_2$, $2C_{18}BGlyPheNH_2$, $2C_{18}BAlaGlyNH_2$, and $2C_{18}BAla_2NH_2$ were synthesized by the pathway given in Scheme 1. Syntheses of $2C_{18}BGly_2NH_2$,[10] dioctadecylamine,[12] and *N*,*N*-dioctadecylterephthalamic acid ($2C_{18}BCOOH$)[10] are described elsewhere. The other chemicals were commercially available. Melting points were recorded on a Yanaco micro melting point apparatus and uncorrected. Chemical shifts of ^{1}H NMR spectra were recorded on a Bruker ARX-300 (300 MHz) spectrometer and are given relative to chloroform (δ 7.26) or tetramethylsilane (δ 0.00). Elemental analyses (C, H, and N) were performed at the Faculty of Science, Kyushu University.

$2C_{18}$BGlyOBn. *N*,*N*-Dioctadecylterephthalamic acid ($2C_{18}BCOOH$; 2.15 g, 3.21 mmol) was dissolved in CH_2Cl_2 (150 mL), and diethyl phosphorocyanidate (DEPC; 0.850 mL, 5.60 mmol) was added to the solution at 0 °C. After stirring for 20 min, glycine benzyl ester−*p*-toluenesulfonic acid salt (TsOH−GlyOBn; 1.31 g, 3.87 mmol) and triethylamine (1.50 mL, 10.8 mmol) dissolved in CH_2Cl_2 (100 mL) were added at 0 °C. The mixture was allowed to react at room temperature for 64.5 h followed by removal of the solvent under reduced pressure. The residue was chromatographed on SiO_2 (3:1 and 1:1 *n*-hexane/EtOAc) to give $2C_{18}BGlyOBn$ as a white solid (2.47 g, 94.1%): mp 59.0−59.5 °C; TLC R_f 0.2 (3:1 *n*-hexane/EtOAc); ^{1}H NMR ($CDCl_3$) δ 0.88 (t, J = 6.6 Hz, 6H, 2 CH_3), 1.26 (br, 60H, 30 CH_2), 1.46−1.65 (br, 4H, 2 CH_2CH_2N), 3.12 (t, J = 7.7 Hz, 2H, CH_2N), 3.47 (t, J = 7.4 Hz, 2H, CH_2N), 4.30 (d, J = 5.0 Hz, 2H, glycine CH_2), 5.24 (s, 2H, $COOCH_2$), 6.72 (br, 1H, amide), 7.35 (s, 5H, $COOCH_2Ph$), 7.41 (d, J = 8.3 Hz, 2H, COPhCO), 7.82 (d, J = 8.2 Hz, 2H, COPhCO). Anal. Calcd for $C_{53}H_{88}N_2O_4$: C, 77.89; H, 10.85; N, 3.43. Found: C, 77.90; H, 10.85; N, 3.46.

$2C_{18}$BGlyOH. Pd/C (Pd 5%, 0.259 g) and $2C_{18}BGlyOBn$ (2.42 g, 2.74 mmol) were dispersed in THF (20 mL) and ethanol (20 mL). The reaction mixture was kept under a H_2 gas atmosphere at room temperature for 7 h. After filtration, the solvents were removed in vacuo. The title compound was obtained as a white solid (1.82 g, 91.7%): mp 111.0−111.5 °C; ^{1}H NMR ($CDCl_3$) δ 0.88 (t, J = 6.6 Hz, 6H, 2 CH_3), 1.25 (br, 60H, 30 CH_2), 1.48−1.66 (br, 4H, 2 CH_2-CH_2N), 3.14 (t, J = 7.2 Hz, 2H, CH_2N), 3.48 (t, J = 7.2 Hz, 2H, CH_2N), 4.11 (d, J = 4.5 Hz, 2H, glycine CH_2), 7.16 (br, 1H, amide), 7.38 (d, J = 8.2 Hz, 2H, aromatic), 7.81 (d, J = 8.1 Hz, 2H, aromatic). Anal. Calcd for $C_{46}H_{82}N_2O_4$: C, 75.98; H, 11.37; N, 3.85. Found: C, 75.80; H, 11.29; N, 3.81.

$2C_{18}$BGlyAlaNH$_2$. $2C_{18}$BGlyOH (0.157 g, 0.228 mmol) was dissolved in CH_2Cl_2 (100 mL), and DEPC (0.070 mL, 0.46 mmol) was added at 0 °C. After stirring for 15 min, L-alaninamide−HBr salt (HBr−$AlaNH_2$; 0.0533 g, 0.315 mmol) and triethylamine (0.150 mL, 1.08 mmol) dissolved in CH_2Cl_2 (50 mL) were added at 0 °C. The mixture was allowed to react at room temperature for 45 h followed by removal of the solvent under reduced pressure. The residue was chromatographed on SiO_2 (1:1 $CHCl_3$/acetone) to give $2C_{18}BGlyAlaNH_2$ as a white solid (0.081 g, 44.8%): mp 135.5−136.0 °C; TLC R_f 0.2 (1:1 $CHCl_3$/acetone); ^{1}H NMR ($CDCl_3$) δ 0.88 (t, J = 6.6 Hz, 6H, 2 CH_3), 1.25 (br, 60H, 30 CH_2), 1.37 (d, J = 7.0 Hz, 3H, alanine CH_3), 1.47−1.65 (br, 4H, 2 CH_2CH_2N), 3.13 (br, 2H, CH_2N), 3.47 (br, 2H, CH_2N), 4.08 (m, 2H, glycine CH_2), 4.35 (m, 1H, alanine α-CH), 5.67 (br, 1H, amide), 6.60 (br, 1H, amide), 7.00 (d, J = 6.9 Hz, 1H, amide), 7.38 (d, J = 8.0 Hz, 2H, aromatic), 7.62 (br, 1H, amide), 7.84 (d, J = 8.1 Hz, 2H, aromatic). Anal. Calcd for $C_{49}H_{88}N_4O_4\cdot{}^1/_3H_2O$: C, 73.27; H, 11.13; N, 6.97. Found: C, 73.24; H, 11.06; N, 6.92.

$2C_{18}$BGlyValNH$_2$. $2C_{18}$BGlyOH (0.099 g, 0.14 mmol) was dissolved in CH_2Cl_2 (100 mL), and DEPC (0.035 mL, 0.23 mmol) was added at 0 °C. After stirring for 20 min, L-valinamide−HCl salt (HCl−$ValNH_2$; 0.0255 g, 0.167 mmol) and triethylamine (0.060 mL, 0.43 mmol) dissolved in CH_2Cl_2 (30 mL) were added at 0 °C. The mixture was allowed to react at room temperature for 77 h followed by removal of the solvent under reduced pressure. The residue was chromatographed on SiO_2 (1:1 $CHCl_3$/acetone) to give $2C_{18}BGlyValNH_2$ as a white solid (0.085 g, 75.9%): mp 206.0−207.0 °C; TLC R_f 0.3 (1:1 $CHCl_3$/acetone); ^{1}H NMR ($CDCl_3$) δ 0.88 (t, J = 6.6 Hz, 6H, 2 CH_3), 0.94 (d, J = 6.9 Hz, 3H, valine CH_3), 0.97 (d, J = 7.0 Hz, 3H, valine CH_3), 1.25 (br, 60H, 30 CH_2), 1.47−1.65 (br, 4H, 2 CH_2CH_2N), 2.18 (m, 1H, valine CH of the side chain), 3.13 (br, 2H, CH_2N), 3.47 (br, 2H, CH_2N), 4.14 (m, 2H, glycine CH_2), 4.30 (m, 1H, valine α-CH), 5.66 (br, 1H, amide), 6.30 (br, 1H, amide), 6.85 (d, J = 8.6 Hz, 1H, amide), 7.40 (d, J = 8.1 Hz, 2H, aromatic), 7.41 (br, 1H, amide), 7.84 (d, J = 8.2 Hz, 2H, aromatic). Anal. Calcd for $C_{51}H_{92}N_4O_4\cdot{}^1/_2H_2O$: C, 73.42; H, 11.24; N, 6.72. Found: C, 73.42; H, 11.20; N, 6.61.

$2C_{18}$BGlyLeuNH$_2$. $2C_{18}$BGlyOH (0.152 g, 0.209 mmol) was dissolved in CH_2Cl_2 (150 mL), and DEPC (0.050 mL, 0.33 mmol) was added at 0 °C. After stirring for 15 min, L-leucinamide−HCl salt (HCl−$LeuNH_2$; 0.0421 g, 0.253 mmol) and triethylamine (0.100 mL, 0.717 mmol) dissolved in CH_2Cl_2 (50 mL) were added at 0 °C. The mixture was allowed to react at room temperature for 44 h followed by removal of the solvent under reduced pressure. The residue was chromatographed on SiO_2 (3:1 and 1:1 $CHCl_3$/acetone) to give $2C_{18}$-$BGlyLeuNH_2$ as a white solid (0.133 g, 76.0%): mp 42.5−43.5 °C; TLC R_f 0.2 (3:1 $CHCl_3$/acetone); ^{1}H NMR ($CDCl_3$) δ 0.88 (t, J = 6.6 Hz, 6H, 2 CH_3), 0.93 (d, J = 6.0 Hz, 3H, leucine CH_3), 0.94 (d, J = 5.8 Hz, 3H, leucine CH_3), 1.25 (br, 60H, 30 CH_2), 1.47−1.74 (br, 7H, 2 CH_2CH_2N + CH and CH_2 in the leucine side chain), 3.13 (t, J = 8.0 Hz, 2H, CH_2N), 3.49 (t, J = 8.0 Hz, 2H, CH_2N), 4.11 (m, 2H, glycine CH_2), 4.47 (m, 1H, leucine α-CH), 5.51 (br, 1H, amide), 6.31 (br, 1H, amide), 6.68 (d, J = 7.7 Hz, 1H, amide), 7.28 (br, 1H, amide), 7.40 (d, J = 8.0 Hz, 2H, aromatic), 7.82 (d, J = 8.1 Hz, 2H, aromatic). Anal. Calcd for $C_{52}H_{94}N_4O_4\cdot{}^1/_2H_2O$: C, 73.62; H, 11.29; N, 6.60. Found: C, 73.69; H, 11.21; N, 6.54.

$2C_{18}$BGlyPheNH$_2$. $2C_{18}$BGlyOH (0.204 g, 0.280 mmol) was dissolved in CH_2Cl_2 (150 mL), and DEPC (0.065 mL, 0.43 mmol) was added at 0 °C. After stirring for 15 min, L-phenylalaninamide−HCl salt (HCl−$PheNH_2$; 0.0627 g, 0.312 mmol) and triethylamine (0.130 mL, 0.932 mmol) dissolved in CH_2Cl_2 (50 mL) were added at 0 °C. The mixture was allowed to react at room temperature for 45 h followed by removal of the solvent under reduced pressure. The residue was chromatographed on SiO_2 (3:1 and 1:1 $CHCl_3$/acetone) to give $2C_{18}$-$BGlyPheNH_2$ as a white solid (0.202 g, 84.0%): mp 91.8−92.3 °C; TLC R_f 0.2 (3:1 $CHCl_3$/acetone); ^{1}H NMR ($CDCl_3$) δ 0.88 (t, J = 6.6 Hz, 6H, 2 CH_3), 1.26 (br, 60H, 30 CH_2), 1.43−1.53 (br, 4H, 2 CH_2-CH_2N), 3.16 (br, 4H, 2 CH_2N), 3.48 (t, J = 6.2 Hz, 2H, Ar-CH_2 in phenylalanine), 4.05 (d, J = 4.8 Hz, 2H, glycine CH_2), 4.67 (m, 1H, α-CH in phenylalanine), 5.46 (br, 1H, amide), 6.03 (br, 1H, amide), 6.75 (br, 1H, amide), 7.13 (br, 1H, amide), 7.23 (m, 5H, aromatic in phenylalanine), 7.40 (d, J = 8.1 Hz, 2H, COPhCO), 7.79 (d, J = 8.4 Hz, 2H, COPhCO). Anal. Calcd for $C_{55}H_{92}N_4O_4\cdot{}^1/_2H_2O$: C, 74.87; H, 10.62; N, 6.35. Found: C, 74.96; H, 10.66; N, 6.08.

(11) Cha, X.; Ariga, K.; Kunitake, T. *Chem. Lett.* **1996**, 73.

(12) Onda, M.; Yoshihara, K.; Koyano, H.; Ariga, K.; Kunitake, T. *J. Am. Chem. Soc.* in press.

$2C_{18}$BAlaOBn. $2C_{18}$BCOOH (0.457 g, 0.682 mmol) was dissolved in CH_2Cl_2 (100 mL), and DEPC (0.150 mL, 0.989 mmol) was added to the solution at 0 °C. After stirring for 20 min, L-alanine benzyl ester−*p*-toluenesulfonic acid salt (TsOH−AlaOBn; 0.283 g, 0.805 mmol) and triethylamine (0.300 mL, 2.15 mmol) dissolved in CH_2Cl_2 (100 mL) were added at 0 °C. The mixture was allowed to react at room temperature for 48 h followed by removal of the solvent under reduced pressure. The residue was chromatographed on SiO_2 (3:1, 1:1, and 1:3 *n*-hexane/EtOAc) to give $2C_{18}$BAlaOBn as a white solid (0.464 g, 81.8%): mp 59.0−59.5 °C; TLC R_f 0.2 (3:1 *n*-hexane/EtOAc); ^{1}H NMR ($CDCl_3$) δ 0.88 (t, J = 6.6 Hz, 6H, 2 CH_3), 1.25 (br, 60H, 30 CH_2), 1.47−1.62 (br, 4H, 2 CH_2CH_2N), 1.54 (d, J = 7.1 Hz, 3H, alanine CH_3), 3.12 (t, J = 7.2 Hz, 2H, CH_2N), 3.47 (t, J = 7.2 Hz, 2H, CH_2N), 4.85 (m, 1H, alanine, α-CH), 5.23 (s, 2H, $COOCH_2$), 6.76 (d, J = 7.2 Hz, 1H, amide), 7.34 (s, 5H, $COOCH_2$*Ph*), 7.41 (d, J = 8.2 Hz, 2H, COPhCO), 7.82 (d, J = 8.3 Hz, 2H, COPhCO). Anal. Calcd for $C_{54}H_{90}N_2O_4$: C, 72.08; H, 10.91; N, 3.37. Found: C, 77.88; H, 10.86; N, 3.34.

$2C_{18}$BAlaOH. Pd/C (Pd 5%, 0.057 g) and $2C_{18}$BAlaOBn (0.508 g, 0.611 mmol) were dispersed in ethanol (10 mL) and THF (10 mL). The mixture was allowed to react under H_2 gas at room temperature for 6 h. After filtration, the solvents were removed in vacuo. The title compound was obtained as a white solid (0.351 g, 77.5%): mp 54.0−55.0 °C; ^{1}H NMR ($CDCl_3$) δ 0.88 (t, J = 6.5 Hz, 6H, 2 CH_3), 1.26 (br, 60H, 30 CH_2), 1.43−1.66 (br, 4H, 2 CH_2CH_2N), 1.54 (d, J = 7.0 Hz, 3H, alanine CH_3), 3.14 (br, 2H, CH_2N), 3.48 (br, 2H, CH_2N), 4.67 (m, 1H, alanine α-CH), 6.84 (d, J = 5.4 Hz, 1H, amide), 7.40 (d, J = 8.1 Hz, 2H, aromatic), 7.80 (d, J = 8.1 Hz, 2H, aromatic). Anal. Calcd for $C_{47}H_{84}N_2O_4$: C, 76.16; H, 11.42; N, 3.78. Found: C, 76.06; H, 11.24; N, 3.68.

$2C_{18}$BAlaGlyNH$_2$. $2C_{18}$BAlaOH (0.146 g, 0.197 mmol) was dissolved in CH_2Cl_2 (150 mL), and DEPC (0.050 mL, 0.33 mmol) was added at 0 °C. After stirring for 15 min, glycinamide−HCl salt (HCl−$GlyNH_2$; 0.0272 g, 0.246 mmol) and triethylamine (0.100 mL, 0.717 mmol) dissolved in dry DMF (10 mL) were added at 0 °C. The mixture was allowed to react at room temperature for 163 h. The organic layer was washed with water and dried over Na_2SO_4 followed by removal of the solvent under reduced pressure. The residue was chromatographed on SiO_2 (1:1 $CHCl_3$/acetone) to give $2C_{18}$BAlaGlyNH$_2$ as a white solid (0.073 g, 46.5%): mp 103.5−104.5 °C; TLC R_f 0.3 (1:1 $CHCl_3$/acetone); ^{1}H NMR ($CDCl_3$) δ 0.88 (t, J = 6.6 Hz, 6H, 2 CH_3), 1.26 (br, 60H, 30 CH_2), 1.47−1.60 (br, 4H, 2 CH_2CH_2N), 1.52 (d, J = 7.1 Hz, 3H, alanine CH_3), 3.13 (br, 2H, CH_2N), 3.47 (br, 2H, CH_2N), 3.70−3.92 (m, 2H, glycine CH_2), 4.59 (m, 1H, alanine α-CH), 5.53 (br, 1H, amide), 6.61 (br, 1H, amide), 6.92 (br, 1H, amide), 7.23 (br, 1H, amide), 7.38 (d, J = 8.2 Hz, 2H, aromatic), 7.81 (d, J = 8.1 Hz, 2H, aromatic). Anal. Calcd for $C_{49}H_{88}N_4O_4 \cdot {}^1/_2H_2O$: C, 73.00; H, 11.13; N, 6.95. Found: C, 72.83; H, 10.99; N, 6.96.

$2C_{18}$BAla$_2$NH$_2$. $2C_{18}$BAlaOH (0.102 g, 0.138 mmol) was dissolved in CH_2Cl_2 (150 mL), and DEPC (0.030 mL, 0.20 mmol) was added at 0 °C. After stirring for 15 min, L-alaninamide−HBr salt (HBr−$AlaNH_2$; 0.0302 g, 0.179 mmol) and triethylamine (0.060 mL, 0.43 mmol) dissolved in CH_2Cl_2 (30 mL) were added at 0 °C. The mixture was allowed to react at room temperature for 163 h. The organic layer was washed with water and dried over Na_2SO_4 followed by removal of the solvent under reduced pressure. The residue was chromatographed on SiO_2 (EtOAc) to give $2C_{18}$BAla$_2$NH$_2$ as a white solid (0.065 g, 58.0%): mp 117.5−118.5 °C; TLC R_f 0.1 (EtOAc); ^{1}H NMR ($CDCl_3$) δ 0.87 (t, J = 6.6 Hz, 6H, 2 CH_3), 1.25 (br, 60H, 30 CH_2), 1.31 (d, J = 7.0 Hz, 3H, alanine CH_3), 1.50 (d, J = 7.0 Hz, 3H, alanine CH_3), 1.51−1.64 (br, 4H, 2 CH_2CH_2N), 3.13 (t, J = 7.1 Hz, 2H, CH_2N), 3.46 (t, J = 7.1 Hz, 2H, CH_2N), 4.06 (m, 1H, alanine α-CH), 4.27 (br, 1H, amide), 4.67 (m, 1H, alanine α-CH), 5.49 (br, 1H, amide), 6.56 (br, 1H, amide), 6.88 (br, 1H, amide), 7.39 (d, J = 8.1 Hz, 2H, aromatic), 7.84 (d, J = 8.1 Hz, 2H, aromatic). Anal. Calcd for $C_{50}H_{90}N_4O_4 \cdot H_2O$: C, 72.42; H, 11.18; N, 6.76. Found: C, 72.34; H, 10.94; N, 6.59.

Surface Pressure−Area (π−A) Isotherms and Langmuir−Blodgett (LB) Films. A computer-controlled film balance system FSD-110 (trough size 100 × 200 mm, USI System, Japan) was used. π−A isotherms were taken at a compression rate of 4 mm·min^{-1} and a subphase temperature of 20.0 ± 0.3 °C. The subphase water was deionized and doubly distilled. The spreading solutions of oligopeptide amphiphiles were ca. 0.16 mg·cm^{-3} in $CHCl_3$. LB films were prepared by using the vertical dipping method at up-stroke and down-stroke motions of 8 and 100 mm·min^{-1}, respectively, from pure water and dipeptide subphases. Monolayers were transferred onto gold-deposited glass slides at a surface pressure of 25 mN·m^{-1}.

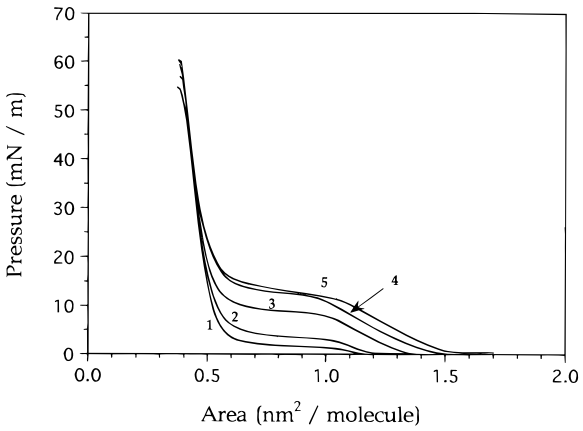

Figure 1. π−A isotherms of $2C_{18}$BGlyYNH$_2$ monolayers at 20.0 ± 0.3 °C on pure water: 1, $2C_{18}$BGly$_2$NH$_2$; 2, $2C_{18}$BGlyAlaNH$_2$; 3, $2C_{18}$BGlyValNH$_2$; 4, $2C_{18}$BGlyLeuNH$_2$; 5, $2C_{18}$BGlyPheNH$_2$.

FT-IR Measurements. Infrared spectra of the LB film on a gold-deposited glass were obtained on an FT-IR spectrometer (Nicolet 710) equipped with a MCT detector (for RAS, reflection absorption spectroscopy). All data were collected by the RAS method at a spectral resolution of 4 cm^{-1}.

XPS Measurement. X-ray photoelectron spectra of the LB films on a gold-deposited glass were measured with a Perkin-Elmer PHI 5300 ESCA instrument (X-ray source Mg Kα, 300 W, scan range 0−1000 eV, takeoff angle 45°). The elemental composition was obtained by dividing the observed peak area by intrinsic sensitivity factors of each element.

Results and Discussion

Monolayer Behavior and Langmuir−Blodgett Transfer. Monolayers of the peptide amphiphiles and mixed monolayers of peptide/benzoic acid amphiphiles (1:1 mole ratio) give analogous surface area−pressure behaviors on pure water. They have expanded phases at low pressures with limiting areas of ca. 0.52−0.55 nm^2 and collapse pressures of 48−58 mN·m^{-1}. Figure 1 summarizes isotherms of single-component monolayers on pure water. All the isotherms have similar molecular areas at the condensed phase, but show different expansion behavior at low pressures. It can be seen that introduction of the hydrophobic side chain in the dipeptide moiety of a host amphiphile leads to expansion of its π−A isotherm at low pressures. The isotherm of $2C_{18}$BGlyPheNH$_2$ has the highest phase transition pressure, while $2C_{18}$BGly$_2$NH$_2$ forms a condensed phase at the lowest pressure. Side chains in these peptide−lipids clearly affect their aggregation behavior. However, the similarity of their limiting areas strongly indicates that the molecular packing at the condensed phase is independent of steric hindrance caused by the side chains.

Figure 2 shows π−A isotherms of mixed monolayers of $2C_{18}$BGly$_2$NH$_2$/$2C_{18}$BCOOH (Figure 2a) and $2C_{18}$BGlyValNH$_2$/$2C_{18}$BCOOH (Figure 2b) at a 1:1 molar ratio on pure water and on aqueous dipeptides (10 mM LeuGly and GlyLeu). The mean molecular areas are used. The mean molecular area of the $2C_{18}$BGly$_2$NH$_2$/$2C_{18}$BCOOH monolayer at 25 mN·m^{-1} on pure water showed 12% positive deviation from that of the ideal mixture calculated as a simple average of the separate single-component monolayers. Therefore, the mixed monolayer is neither ideally mixed nor phase separated. The interlipid

Table 1. Binding Ratios of Dipeptides toward 1:1 Mixed and Single-Component Monolayer as Determined by XPS[a]

monolayer		Guest/Host (mol/mol)[b]						
peptide component	second component	GlyLeu	LeuGly	AlaPhe	PheAla	LeuPhe	LeuLeu	GlyGly
$2C_{18}BGly_2NH_2$	$2C_{18}BCOOH$	0.41	0.45	0.60	0.42	0.33	0.45	0.00
$2C_{18}BGlyAlaNH_2$	$2C_{18}BCOOH$	0.36		0.27		0.09	0.00	
$2C_{18}BGlyValNH_2$	$2C_{18}BCOOH$	0.34	0.35	0.00		0.05	0.00	0.39
$2C_{18}BGlyLeuNH_2$	$2C_{18}BCOOH$	0.14						
$2C_{18}BGlyPheNH_2$	$2C_{18}BCOOH$	0.00						
$2C_{18}BAlaGlyNH_2$	$2C_{18}BCOOH$	0.38						
$2C_{18}BAla_2NH$**2**	$2C_{18}BCOOH$	0.41						
$2C_{18}BGly_2NH_2$		0.33	0.00				0.00	
$2C_{18}BCOOH$		0.17	0.17				0.00	0.00

[a] LB films of 14 layers were used. [b] The concentration of the aqueous guest was 0.01 M.

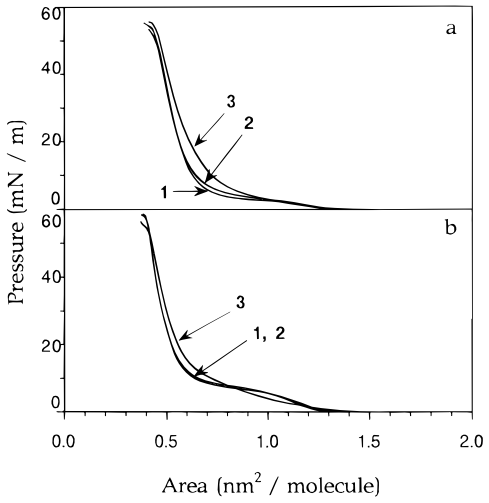

Figure 2. (a) $\pi-A$ isotherms of a $2C_{18}BGly_2NH_2/2C_{18}BCOOH$ mixed monolayer (1:1 mole ratio) at 20.0 ± 0.3 °C: 1, on pure water; 2, on 0.01 M LeuGly; 3, on 0.01 M GlyLeu. (b) $\pi-A$ isotherms of a $2C_{18}BGlyValNH_2/2C_{18}BCOOH$ mixed monolayer (1:1 mole ratio) at 20.0 ± 0.3 °C: 1, on pure water; 2, on 0.01 M LeuGly; 3, on 0.01 M GlyLeu.

hydrogen bonding in the $2C_{18}BGly_2NH_2$ monolayer is apparently broken by mixing with the $2C_{18}BCOOH$ molecule, which causes the positive deviation in the molecular area.

Although the structural difference in peptide side chains does not alter the limiting area, the presence of aqueous peptides clearly affects molecular packing in the mixed monolayer even at the condensed phase. This is indicated by the expansion of the $\pi-A$ isotherms in Figure 2. Interestingly, the expansion is influenced by the type of aqueous dipeptides. The $\pi-A$ behavior of the two mixed monolayers were little affected by 10 mM LeuGly relative to those on pure water, but the isotherms show expansion on 10 mM GlyLeu. Thus, the monolayer/dipeptide interaction is specific to the dipeptide structure.

Monolayers were transferred onto a gold-deposited glass plate at a surface pressure of 25 $mN\cdot m^{-1}$. Single-component peptide monolayers showed varied transfer behavior. The monolayers of $2C_{18}BGly_2NH_2$, $2C_{18}BGlyAlaNH_2$, and $2C_{18}BAla_2NH_2$ showed Y type transfer behavior, while the monolayers of $2C_{18}BGlyValNH_2$, $2C_{18}BGlyLeuNH_2$, and $2C_{18}BGlyPheNH_2$ were transferred in the Z mode. Only the $2C_{18}BAlaGlyNH_2$ monolayer showed unsuccessful transfer due to return of the transferred monolayer to water in the down-stroke motion.

All the mixed monolayers were successfully transferred onto a gold-deposited glass plate at 25 $mN\cdot m^{-1}$. The transfer ratio from pure water and from the aqueous dipeptide subphase was 1.0 ± 0.1 in the up-stroke mode in all cases, but the ratio was varied in the down-stroke motion, depending on the hydrophobicity of the guest peptides and polar groups of the host molecules. For example, no transfer was observed for monolayers of $2C_{18}BGly_2NH_2/2C_{18}BCOOH$ in the down-stroke mode on the subphases of 0.01 M GlyLeu, GlyPhe, LeuGly, and PheGly, while the ratio was (0.2−0.4) ± 0.1 for pure water. Generally, the transfer ratio in the down-stroke mode decreased in the presence of dipeptides.

Selectivity in Dipeptide Binding. The binding behavior of dipeptides to the monolayers is summarized in Table 1. The host/guest ratios are given for a 0.01 M guest concentration. Our previous studies established that the $2C_{18}BGly_2NH_2$ monolayer can bind aqueous dipeptides of GlyX type only.[10] Other dipeptide monolayers of $2C_{18}BGlyYNH_2$ (Y = Ala, Val, Leu, and Phe) did not bind aqueous dipeptides efficiently. Clearly, the amino acid residue larger than Gly in $2C_{18}BGlyYNH_2$ amphiphiles cannot provide proper binding cavities in their single-component monolayers. The $2C_{18}BCOOH$ monolayer is similarly not capable of efficient binding of aqueous dipeptides. For example, the binding ratios of GlyLeu, LeuGly, LeuLeu, and GlyGly toward the $2C_{18}BCOOH$ monolayer are 0.17, 0.17, 0.00, and 0.00, respectively. In contrast, the equimolar mixture of $2C_{18}BGly_2NH_2/2C_{18}BCOOH$ can bind both GlyX and XGly dipeptides, and it can even bind XX′ dipeptides which have large side chains on both of the two amino acid residues.

The binding efficiency depends on the combination of monolayer components. As shown in Table 1, their binding is lessened or is lost with increasing sizes of the side chain of the dipeptide moiety in the host molecules. The binding ratio of GlyLeu is 0.41 to the $2C_{18}BGly_2NH_2/2C_{18}BCOOH$ monolayer, while GlyLeu is hardly bound to $2C_{18}BGlyPheNH_2/2C_{18}BCOOH$. Most of dipeptides except for small GlyGly show higher affinities to $2C_{18}BGly_2NH_2/2C_{18}BCOOH$ monolayers than to $2C_{18}BGlyValNH_2/2C_{18}BCOOH$. The aqueous dipeptide binding is also lessened or lost with increasing sizes of the guest dipeptides. For example, binding ratios of LeuPhe and LeuLeu to the $2C_{18}BGlyAlaNH_2/2C_{18}BCOOH$ monolayer are 0.09 and 0.00, respectively, while those of GlyLeu and AlaPhe are around 0.3. A similar tendency was observed in the case of the $2C_{18}BGlyValNH_2/2C_{18}BCOOH$ monolayer. In contrast, slim GlyGly shows a higher binding affinity to $2C_{18}BGlyValNH_2/2C_{18}BCOOH$ than to the $2C_{18}BGly_2NH_2/2C_{18}BCOOH$ monolayer. These facts imply that size matching between the guest molecule and host cavity is required for effective binding.

The binding ratios of GlyLeu to monolayers of $2C_{18}BGlyAlaNH_2/2C_{18}BCOOH$, $2C_{18}BAlaGlyNH_2/2C_{18}BCOOH$, and $2C_{18}BAla_2NH_2/2C_{18}BCOOH$ are 0.36, 0.38, and 0.41, respectively. These close ratios indicate that the nature of the binding cavity is not significantly altered by the replacement of Ala and Gly residues in the host molecules for the GlyLeu guest.

Saturation and Stoichiometry of Dipeptide Binding. The binding behavior of GlyLeu to $2C_{18}BGly_2NH_2/2C_{18}BCOOH$ monolayer was examined more closely to determine binding parameters. The molar ratio of the bound guest per lipid is plotted as a function of guest concentration in Figure 3. The

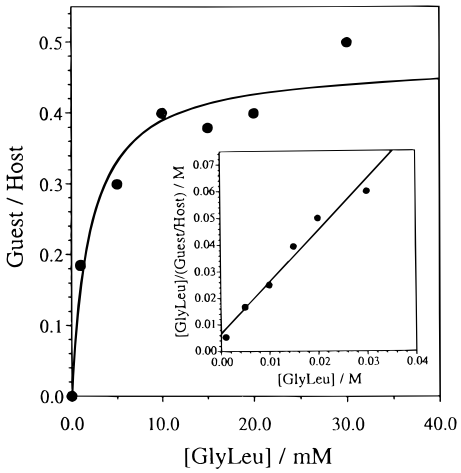

Figure 3. Binding curve of GlyLeu to an equimolar mixed monolayer of $2C_{18}BGly_2NH_2/2C_{18}BCOOH$. The inset represents Langmuir plots of GlyLeu as described in eq 1.

plots show saturation behavior, indicating that the monolayer provides a specific binding site. The plots were analyzed by using the Langmuir isotherm:

$$[S]/y = 1/(\alpha K) + [S]/\alpha \qquad (1)$$

where y is the guest/host ratio, [S] is the guest concentration in the subphase, α is the saturation binding ratio, and K is the binding constant. The plots show binding saturation at more than 10 mM aqueous guest, suggesting that the recognition is site-specific. Curve fitting of the plots gives a site occupancy (i.e., the guest/host ratio at saturation) of 0.47 and a binding constant of 475 M^{-1}. The α value observed indicates that one GlyLeu molecule is bound to two monolayer molecules. This behavior is different from the equimolar site occupancy observed for the single-component monolayer of $2C_{18}BGly_2NH_2$ with the same guest. The magnitude of K is also different. The binding constant with the mixed monolayer is much larger than that with the $2C_{18}BGly_2NH_2$ single-component monolayer ($K = 35$ M^{-1}).[10]

FT-IR Investigation of the Host Structure of Mixed Monolayers. FT-IR spectra in the reflection−absorption mode of LB films of monolayers of $2C_{18}BCOOH$ and $2C_{18}BGlyValNH_2/2C_{18}BCOOH$, both transferred from pure water, are shown in Figure 4 (1200−1800 cm^{-1} region) and Figure 5 (2450−2800 cm^{-1} region). The $2C_{18}BCOOH$ film from pure water (Figures 4a and 5a) shows strong peaks characteristic of the hydrogen-bonded dimer of benzoic acid (1697 ($\nu_{C=O}$ (dimeric COOH)), 2543 and 2666 cm^{-1} (ν_{OH}, (dimeric COOH)) and a very weak peak of non-hydrogen-bonded COOH (1721 cm^{-1}, $\nu_{C=O}$). It means that self-hydrogen-bonding is formed in the $2C_{18}BCOOH$ film. On the contrary, in the spectrum of $2C_{18}BGlyValNH_2/2C_{18}BCOOH$ LB film (Figures 4b and 5b), these characteristic peaks at 1697, 2543, and 2665 cm^{-1} disappear and the peak of monomeric COOH (1721 cm^{-1}) becomes stronger. Therefore, the two components in the monolayer are mixed well with each other without phase separation. The microdomain formation of $2C_{18}BCOOH$, if any, would produce self-association of COOH groups. The peptide head group of amphiphile $2C_{18}BGlyValNH_2$ probably hinders formation of the COOH dimer even when the monolayer is transferred in the Y mode. Other characteristic peaks, amide I (1656−1678 cm^{-1}, overlapped) and amide II (1545 cm^{-1}) from $2C_{18}BGlyValNH_2$, are also observed.

Similar spectral characteristics are found in the $2C_{18}BGly_2NH_2/2C_{18}BCOOH$ system (spectra not shown). FT-IR spectra of the individual components show characteristics of intermolecular hydrogen bonding (dimeric COOH for the $2C_{18}BCOOH$ monolayer with $\nu_{C=O}$ at 1701 cm^{-1}, and hydrogen-bonded oligoglycine units for the $2C_{18}BGly_2NH_2$ monolayer with ν_{NH} at 3309 cm^{-1}). In the mixed monolayer, the ν_{NH} peak is shifted to 3320 cm^{-1}, and the COOH peak becomes a broadened shoulder at 1700−1720 cm^{-1}. These IR features indicate that intermolecular hydrogen bonds among the individual components are destroyed due to mixing of the two components. This observation is consistent with the positive deviation in molecular area upon mixing of the two components.

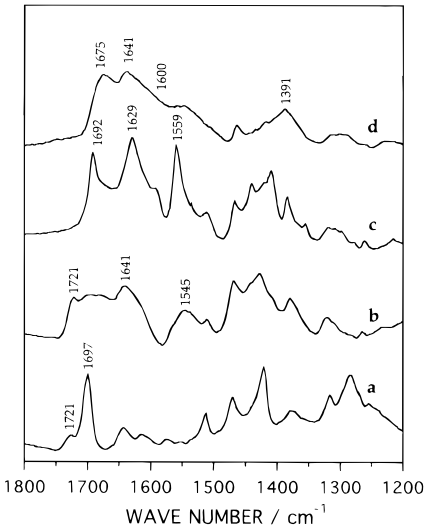

Figure 4. FT-IR−RAS spectra (1200−1800 cm^{-1}) of LB films (15 layers): a, a $2C_{18}BCOOH$ monolayer transferred from pure water; b, a $2C_{18}BGlyValNH_2/2C_{18}BCOOH$ equimolar monolayer transferred from pure water; c, a $2C_{18}BGlyValNH_2/2C_{18}BCOOH$ equimolar monolayer transferred from 0.03 M GlyLeu; d, a $2C_{18}BGlyValNH_2/2C_{18}BCOOH$ equimolar monolayer transferred from 0.03 M LeuGly.

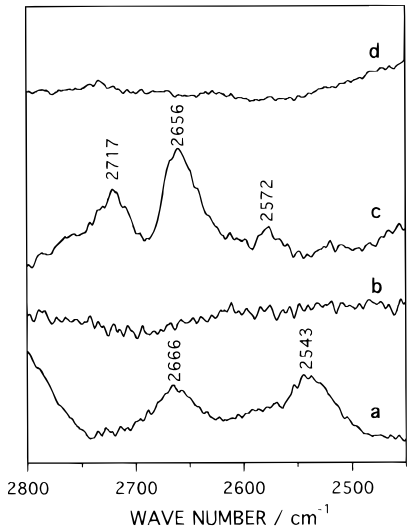

Figure 5. FT-IR−RAS spectra (2450−2800 cm^{-1}) of LB films (15 layers): a, a $2C_{18}BCOOH$ monolayer transferred from pure water; b, a $2C_{18}BGlyValNH_2/2C_{18}BCOOH$ equimolar monolayer transferred from pure water; c, a $2C_{18}BGlyValNH_2/2C_{18}BCOOH$ equimolar monolayer transferred from 0.03 M GlyLeu; d, a $2C_{18}BGlyValNH_2/2C_{18}BCOOH$ equimolar monolayer transferred from 0.03 M LeuGly.

FT-IR Investigation of the Host−Guest Interaction. A mixed monolayer of $2C_{18}BGlyValNH_2/2C_{18}BCOOH$ shows different IR characteristics when transferred from 0.03 M aqueous GlyLeu (Figures 4c and 5c). We can see strong characteristic peaks of the dimeric COOH at 1692, 2572, 2656, and 2717 cm^{-1}, and characteristic peaks of amide I at 1629 and amide II at 1559 cm^{-1} (from the guest peptide). Only a

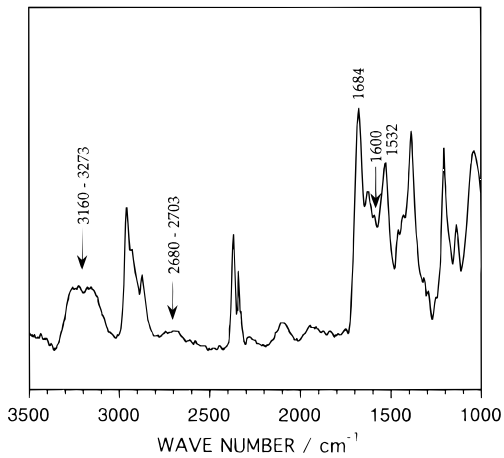

Figure 6. FT-IR−RAS spectrum of a $2C_{18}BGly_2NH_2/2C_{18}BCOOH$ equimolar monolayer transferred from 0.03 M LeuLeu in the region of 1000−3500 cm^{-1}.

small characteristic peak due to salt bridge formation between host COO^- and guest NH_3^+ is detected in the region between amide I and amide II. The free COOH peak is also not found at 1721 cm^{-1}. These results suggest that guest GlyLeu mainly forms a COOH dimer at its C-terminal with the benzoic acid group of the $2C_{18}BCOOH$ amphiphile.

In the case of $2C_{18}BGlyValNH_2/2C_{18}BCOOH$ transferred from 0.03 M aqueous LeuGly, a characteristic peak for monomeric COOH at 1721 cm^{-1} disappears, and peaks for dimeric COOH are absent in the regions of 1680−1700 and 2500−2700 cm^{-1} (Figures 4d and 5d). These facts strongly indicate that the interaction between the host monolayer and guest LeuGly do not contain formation of the COOH dimer. In contrast, a large overlapped shoulder occurs at around 1600 cm^{-1} between the amide I and amide II peaks of the host, which usually represents existence of COO^- and NH_3^+. Therefore, the salt bridge may be formed between the carboxylate of the host monolayer and the N-terminal NH_3^+ of the guest dipeptide upon N-terminal guest insertion. In addition, hydrogen bonding between amide groups is implied by the absence of the free ν_{NH} peak (data not shown).

On the other hand, LeuLeu appears to be inserted into the monolayer of $2C_{18}BGly_2NH_2/2C_{18}BCOOH$ at both of the C- and N-terminals. As shown in Figure 6, a characteristic peak of amide II from guest LeuLeu is found at 1532 cm^{-1}. A peak corresponding to formation of a salt bridge of COO^- (from the monolayer) and NH_3^+ (from LeuLeu) is observed at about 1600 cm^{-1}. At the same time, a broad peak corresponding to dimeric COOH is found at 2680−2703 cm^{-1}, and suggests interaction of the monomeric benzoic acid with the C-terminal of LeuLeu. A strong peak at 1684 cm^{-1} may be attributed to overlapped peaks of dimeric COOH (it is usually located at 1690−1705 cm^{-1}) in the C-terminal insertion mode and of hydrogen-bonded COOH with the host amide (it is usually at 1676−1650 cm^{-1}) in the N-terminal insertion mode.

Binding Mechanism of Dipeptides. Schematic representations of the receptor sites are summarized in Figure 7. Key factors for dipeptide binding are cavity size, mode of hydrogen bonding, and disposition of the guest hydrophobic group.

Monolayers of single-chain derivatives of oligoglycines formed strong inter-peptide hydrogen bonding among component amphiphiles, and binding of guest peptides was not detectable. Formation of the inter-peptide hydrogen bonds probably destroys molecular space needed for peptide insertion, and free amide groups are not available for guest binding (Figure 7a).[9]

The single-component monolayer of $2C_{18}BGly_2NH_2$ showed a selective binding capability toward GlyX.[10] Combination of a bulky double alkyl chain and a smaller Gly_2NH_2 unit can produce a suitable cavity for dipeptide binding at the interface. Binding of GlyX with C-terminal insertion is promoted by formation of antiparallel hydrogen bonds and incorporation of the guest hydrophobic chains into the hydrophobic side of the host monolayer (Figure 7b). Binding of XGly in N-terminal insertion that can bring guest hydrophobic groups into the hydrophobic region of monolayer receptors is not favored, because this mode can only form less stable parallel hydrogen bonds. This difference in the stability of hydrogen bonding would result in selective binding of GlyX to the $2C_{18}BGly_2NH_2$ monolayer. These examples indicate the importance of the mode of hydrogen bonding for the dipeptide binding.

Dipeptide binding was not observed in the case of single-component oligopeptide monolayers of $2C_{18}BGlyYNH_2$ (Y = Ala, Val, Leu, and Phe). Since molecular areas of these monolayers in the condensed phase are almost the same as that of $2C_{18}BGly_2NH_2$ (Figure 1), lipids with a large side chain cannot provide cavities large enough for insertion of guest dipeptides. The nature of the binding cavity can be readily modified by using mixed monolayers. The binding to mixed monolayers of $2C_{18}BXYNH_2/2C_{18}BCOOH$ was detected for some dipeptides. The binding behavior depends on the size of the side chains of the amino acid residues in both the dipeptide guests and peptide monolayer hosts (see Table 1). Combination of a large guest and a large host, for example, a LeuLeu guest and a $2C_{18}BGlyValNH_2/2C_{18}BCOOH$ host, and that of a small guest and a small host, for example, a GlyGly guest and a $2C_{18}BGly_2NH_2/2C_{18}BCOOH$ host, did not produce effective binding. In contrast, complementary combinations of large guest/small host, e.g., LeuLeu and $2C_{18}BGly_2NH_2/2C_{18}BCOOH$, and of small guest/large host, e.g., GlyGly and $2C_{18}BGlyValNH_2/2C_{18}BCOOH$, showed significant binding. These facts imply that size matching based on van der Waals contact between the cavity and guest is essential for effective binding. A plausible model of incorporation of GlyLeu into the receptor site of the $2C_{18}BGlyValNH_2/2C_{18}BCOOH$ monolayer is depicted in Figure 7c. In this model, aqueous GlyLeu is bound to the monolayer from its C-terminal by forming hydrogen-bonded dimeric COOH with the host benzoic acid. The hydrophobic side chain of GlyLeu faces the hydrophobic part of the monolayer. Antiparallel hydrogen bonding is formed with surrounding dipeptide moieties of the host molecules.

In contrast, aqueous LeuGly is bound to the monolayer of $2C_{18}BGlyValNH_2/2C_{18}BCOOH$ from its N-terminal (Figure 7d). FT-IR spectra indicated formation of a carboxylate/ammonium salt bridge at about 1600 cm^{-1}. We suspected that XGly dipeptides could not bind to the single-component monolayer of $2C_{18}BGly_2NH_2$ because the anticipated parallel hydrogen bonding is not sufficiently strong. However, the formation of the salt bridge at the N-terminal of the guest can supply additional host−guest interaction and probably compensates the disadvantage of the parallel hydrogen bonding. The hydrophobic interaction that is expected in this model between the hydrophobic side chain of LeuGly and the hydrophobic part of the monolayer would also contribute to effective binding.

Induction of a Recognition Site by Guest Binding. The experimental results presented here have an important implication for the formation of receptor sites. Two monolayer components, $2C_{18}BGly_2NH_2$ and $2C_{18}BCOOH$, are mixed well on pure water. This is clear from the positive deviation in the molecular area and the IR spectral data of the mixed monolayer. Specific interaction of these two components is not supported

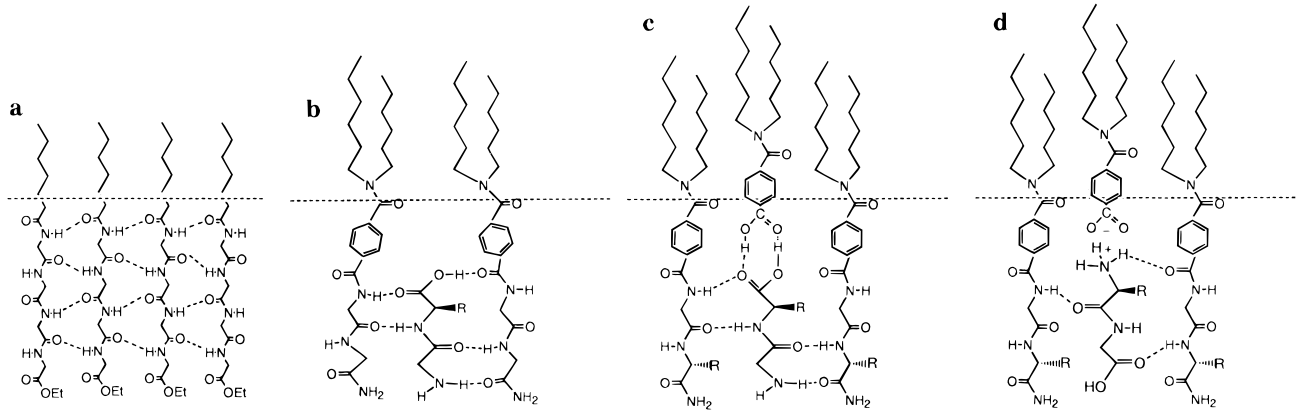

Figure 7. Schematic representation of binding modes of aqueous peptides to peptide-functionalized monolayers: a, a monolayer of a single-chain oligoglycine amphiphile; b, a monolayer of a double-chain oligoglycine amphiphile ($2C_{18}BGly_2NH_2$) with GlyX by C-terminal insertion: c, a 1:1 mixed monolayer of $2C_{18}BGlyValNH_2/2C_{18}BCOOH$ with GlyX by C-terminal insertion; d, a 1:1 mixed monolayer of $2C_{18}BGlyValNH_2/2C_{18}BCOOH$ with XGly by N-terminal insertion. The dotted lines represent hydrogen bonds.

by the available data, and therefore, they must be mixed randomly on pure water. In contrast, a specific 2:1 interaction (two host and one guest molecules) between the host monolayer of $2C_{18}BGly_2NH_2/2C_{18}BCOOH$ and the guest GlyLeu is observed, as suggested by the Langmuir adsorption isotherm. The guest binding must induce redistribution of monolayer components so as to produce a specific binding site. Thus, the binding site is created through the "induced-fit" mechanism. The induced-fit concept was first proposed by Koshland: binding of substrates to an enzyme active site causes conformational changes that align the catalytic groups in their correct orientation.[13] A similar situation appears to exist for the mixed monolayer. This conclusion points to an interesting possibility. Mixed monolayers with suitable lipid combinations would create receptor sites appropriate for different guest molecules through the induced-fit mechanism. This combinatorial recognition site is crudely analogous to the hypervariable region of antibodies.[14] We believe that the existence of flexible recognition sites is characteristic of mixed monolayers. As we reported already, three functional components in mixed monolayers can bind specifically to one molecule of flavin adenine dinucleotide (FAD) at the air−water interface.[15−17] The three monolayer components appear to be statistically mixed in the absence of aqueous FAD, but are organized regularly via specific interactions with FAD molecules.

JA961526F

(13) Koshland, D. E., Jr.; Neméthy, G.; Filmer, D. *Biochemistry* **1971**, *5*, 365.

(14) Capra, J. D. *Sci. Am.* **1977**, *236*, 50.

(15) Taguchi, K.; Ariga, K.; Kunitake, T. *Chem. Lett.* **1995**, 701.

(16) Oishi, Y.; Torii, Y.; Kuramori, M.; Suehiro, K.; Ariga, K.; Taguchi, K.; Kamino, A.; Kunitake, T. *Chem. Lett.* **1996**, 411.

(17) Oishi, Y.; Torii, Y.; Kato, T.; Kuramori, M.; Suehiro, K.; Ariga, K.; Taguchi, K.; Kamino, A.; Koyano, H.; Kunitake, T. *Langmuir*, submitted for publication.